American Mineralogist, Volume 71, pages 78–84, 1986

Morphologies and growth mechanisms of synthetic Mg-chlorite and cordierite

MOONSUP CHO[1]

Department of Geology, University of Toronto, Toronto, Ontario M5S 1A1, Canada

AND J. J. FAWCETT

Department of Geology and Division of Sciences, Erindale College University of Toronto, Toronto, Ontario M5S 1A1, Canada

Abstract

SEM studies have been conducted to investigate the crystal morphologies and growth mechanisms of chlorite and cordierite, which were synthesized using oxide mixtures of clinochlore composition as starting material at 2 kbar water pressure.

7 Å chlorite grows first by three-dimensional nucleation and subsequently by layer growth. With increasing run duration, 14 Å chlorite appears and grows initially by development of successive layers followed by Frank's spiral mechanism. Cordierite grows as large (40 to 400 μm) euhedral grains through prior formation of an acicular or slender prismatic form that may be high cordierite.

Introduction

In the preceding paper (Cho and Fawcett, 1986) we have presented the results of our kinetic study of the Mg-chlorite composition $5MgO \cdot Al_2O_3 \cdot 3SiO_2 \cdot 4H_2O$ involving 7 Å chlorite, clinochlore and its high-temperature equivalent, the assemblage forsterite–cordierite–spinel. A time–temperature–transformation (TTT) diagram was established for the 600° to 750°C temperature interval at 2 kbar P_{H_2O} for periods up to 249 days.

In the present study, all the products of synthesis experiments were examined with a scanning electron microscope to investigate the crystal morphologies and growth mechanisms of Mg-chlorite and cordierite as a function of temperature and experiment duration. Other phases encountered in the synthesis experiments were not thoroughly studied because of their very fine grain size, less than a few μm for spinel and forsterite, or because of the low abundance (talc). Several workers have recently investigated the growth mechanisms of sheet silicates: e.g., synthetic phlogopite (Baronnet, 1972, 1978); natural chlorite, white mica and the kaolin group minerals (Sunagawa, 1981). Although Sunagawa and his colleagues have attempted to document the growth morphologies of natural chlorites from different geologic environments, no experimental studies have attempted to examine the growth mechanisms of synthetic chlorite. For the growth morphologies of cordierite, the only work available to our knowledge is that of Venkatesh (1952), who has described morphological variations in natural cordierite. This study documents the morphology and growth mechanisms of synthetic chlorite and cordierite obtained in experiments of different duration in the temperature ranges 600 to 690°C (chlorite) and 712 to 744°C (cordierite) at 2 kbar P_{H_2O}. Preliminary results of the present investigation were given by Cho and Fawcett (1982).

Experimental technique

Experiments were conducted using conventional cone-in-cone cold seal pressure vessels (Tuttle, 1949) at $T = 600$–750°C and $P = 2$ kbar water pressure. Chlorite and cordierite bearing assemblages were produced in experiments varying from 10 minutes to 249 days duration. The starting material for all experiments in this study was an oxide mixture of clinochlore composition ($5MgO \cdot Al_2O_3 \cdot 3SiO_2$). Details concerning the experimental procedures and the calibration of temperature and pressure are described in the preceding paper (Cho and Fawcett, 1986).

The scanning electron microscope (SEM) was used to determine the morphological changes and identify growth mechanisms of synthetic Mg-chlorite and cordierite. All run products containing either 7 Å or 14 Å chlorite, or cordierite were examined with a Cambridge Instruments Stereoscan Mark IIa SEM and some by a Stereoscan 180 SEM. Phases were identified using a Si(Li) X-ray detector by visually comparing unknown and known spectra.

Run products were prepared for SEM study by filing through the sharp edge of the flattened capsule and then peeling away the capsule. Most of the run products except for those of higher temperature assemblages were easily extracted and then mounted on SEM stubs in their original shapes. However, the higher temperature assemblages, especially, forsterite–cordierite–spinel, were so fragile and friable that a good conductive coating was not

[1] Present address: Department of Geology, Stanford University, Stanford, California 94305.

0003–004X/86/0102–0078$02.00

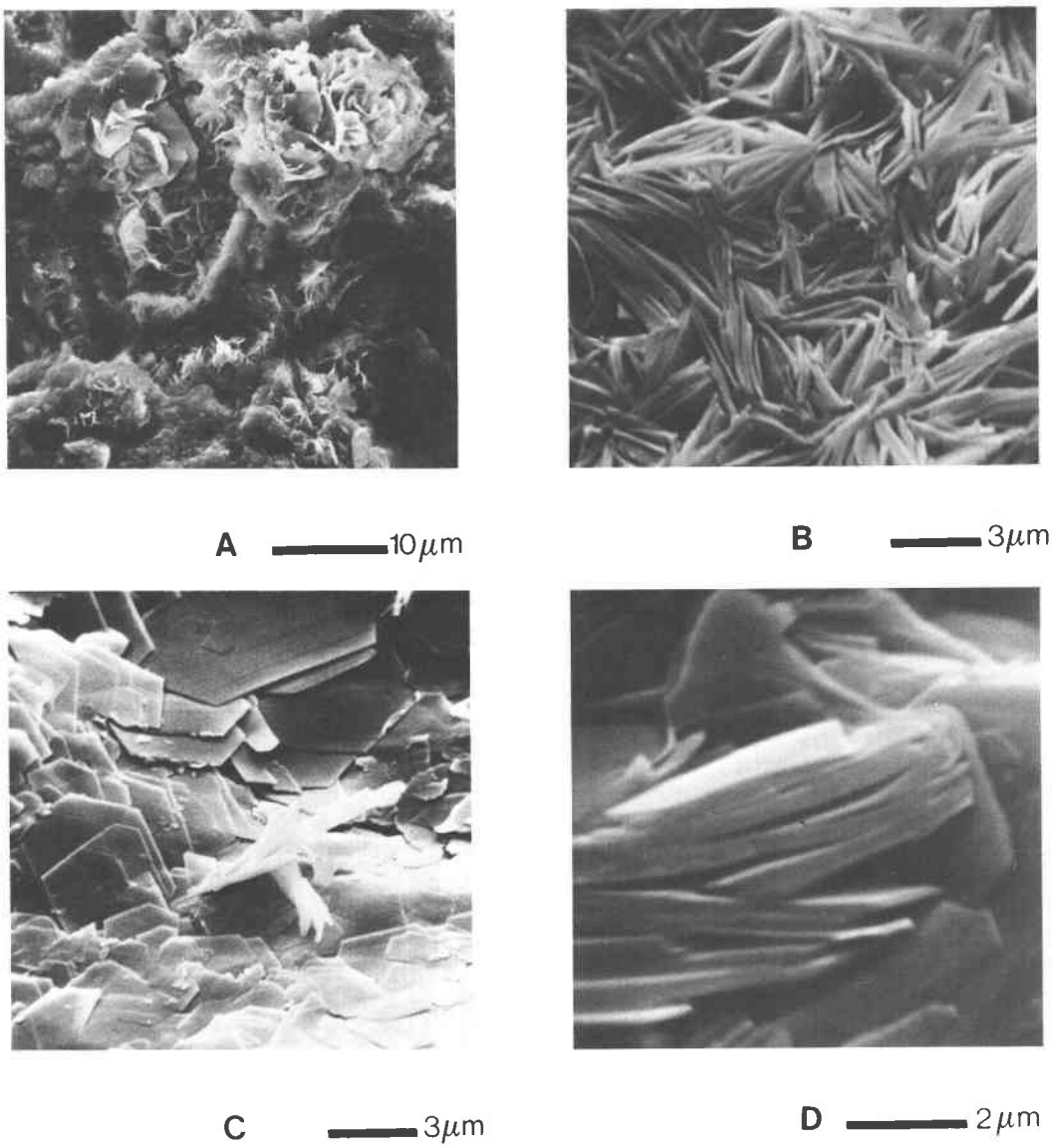

Fig. 1. SEM photomicrographs showing growth features of chlorite at 600 to 650°C. (A) 7 Å chlorite flakes occurring within the inner portion of run product (600°C, 1 hour). (B) Typical rosette-like aggregate of 7 Å chlorite. Note many pores closely associated with chlorite plates (600°C, 72 days). (C) Well-crystallized chlorite hexagons which are found on the surface of run product. The size of chlorite ranges from 1.7 to 9.2 μm. White phase in the center is an impurity attached to the surface during sample preparation (650°, 3 days). (D) Oblique stacking of chlorite layers (625°, 72 days).

achieved. This resulted in charging problems and poor quality photographs.

Morphology and growth of chlorite

In general, the features produced at lower temperatures (i.e., 600 to 650°C) were also observed in the shorter duration experiments at 690°C. Only the 690°C results show a complete progression in chlorite morphological development. At 600°C unreacted oxide mixture occurs with 7 Å chlorite and metastable forsterite even after 72 days. The 14 Å reflection from chlorite appears only in the 140 day experiment at this temperature. Figure 1 shows growth features observed in runs at 600 to 650°C.

At all temperatures the short duration experiments produce poorly crystallized platelets of chlorite (Fig. 1A). The surface energy of the sample container results in a markedly increased grain size in a very narrow (5 μm) outer rim of the sample (Fig. 1C). Consequently neither the average nor maximum grain size of the sample can be directly correlated with experimental duration.

In shorter runs of 10 minutes to 1 day duration, at 690°C chlorite platelets less than 5 μm in size occur as aggregates within a finer grained oxide mixture. It rarely occurs as hexagonal plates and is mainly subhedral and anhedral. Furthermore, no growth layers are found on the basal plane of chlorite. Thus the first stage of growth in these

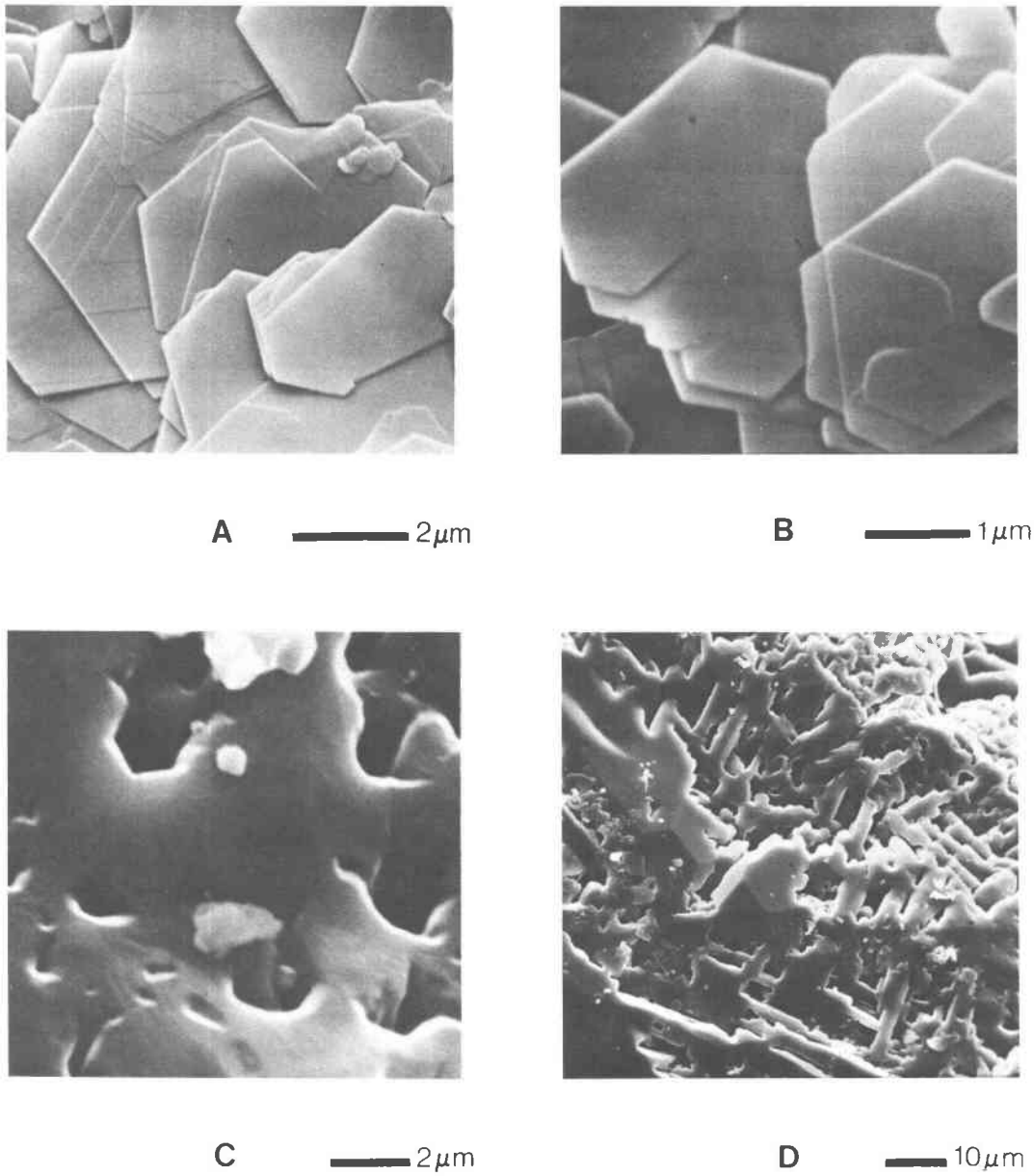

Fig. 2. SEM photomicrographs showing growth features of chlorite and cordierite. (A) Dislocation-controlled growth spirals developing on the basal plane of chlorite. Each chlorite plate also appears to develop in a clockwise direction, resulting in a circular shape as a whole (140 days, 690°C). (B) Co-operating spirals of same hands on the basal plane of chlorite (140 days, 690°C). (C) Irregular basal plane of cordierite, showing growth pits. Some pits are filled by later growth (left bottom). Note the enclosure of very-fine grain size (spinel?) in a pseudohexagonal pit (712°C, 72 days). (D) Intersecting growth pits, resulting from skeletal growth of cordierite (721°C, 22 days).

runs can be ascribed to the mechanism of three-dimensional nucleation or growth islands and later to the layer-growth mechanism. Since no growth steps are observed even at high magnifications (20000×), the lateral growth rate of the nucleus is faster than the nucleation frequency on the (001) face.

In a 3 day run at 690°C the morphology of chlorite is quite different. It shows euhedral, pseudohexagonal platelets with the edges of growth layers parallel to the external edges of the crystal. In longer runs (up to 72 days), these growth layers are also commonly observed. In addition, multiple seeds are frequently observed to coexist in the same face. Therefore, the layer-growth mechanism, in which the lateral growth rate is slower than the nucleation frequency on the basal face, played a major role in the growth of chlorite at this stage.

The diameter of individual chlorite crystals varies from one micron to ten microns in runs longer than three days.

It does not increase or decrease with increasing run duration. However, the plate thickness does increase with run duration and reaches 0.3 μm in a run of 72 days. This later growth of chlorite parallel to the c-axis follows from the Bravais law—i.e., growth is fastest in the direction with the smallest lattice spacing. It may also be inferred that the basal planes have the lowest surface energy (Franchini-Angela and Aquilano, 1984). Thus, given the appropriate range of supersaturation or run duration, two-dimensional nucleation and growth will occur on the edges but not on the basal planes (Pamplain, 1975).

In a 140 day run, distinct spirals with exposed edges are commonly observed for the first time (Fig. 2A, B). These spirals are well-polygonized and exhibit classic interaction patterns (Verma, 1953), such as two spirals of opposite hand, forming closed loops and two cooperating spirals of the same hand (Fig. 2B). The occurrence of growth spirals is limited to the longer runs, indicating that chlorite grows finally by the dislocation controlled spiral-growth mechanism. The inner and outer portions of the run product are distinctly different. Near the surface chlorite crystals are up to 10 μm in diameter and show spiral growth features, while in the interiors the maximum grain size is limited to 3 μm and spiral growth is absent. The large difference in grain size and growth mechanism of chlorite between the two regions indicate that nucleation and growth rates are smaller in the inner portions than near the surface of the run product.

Discussion

The growth mechanisms of basal faces in synthetic micas were summarized by Baronnet (1972, 1978). He concluded that synthetic phlogopite grows by Frank's spiral mechanism after an initial layer-by-layer growth mechanism and that growth spirals are polygonized in short runs, becoming rounded after 30 days run duration. For the growth mechanism of natural chlorite, Sunagawa (1977) reported that, "In contrast to the common occurrence of hydrothermal and metasomatic origins, those occurring in metamorphic rocks do not usually show growth spirals. They are characterized by closed loops of smooth layers with narrow spacings or jagged saw-tooth like steps."

The growth mechanisms of synthetic chlorite described in the previous sections are almost equivalent to those observed in synthetic hydroxyl-phlogopite (Baronnet, 1972). These can be divided into three stages: (1) three-dimensional nucleation or the growth-islands mechanism; (2) two-dimensional nucleation or layer growth mechanism; and (3) spiral growth mechanism. Neither the interlacing nor the general rounding of spirals observed in later growth stages of synthetic phlogopite are found.

7 Å chlorite appears initially as extremely thin plates commonly in rosette-like aggregates resulting from three-dimensional nucleation and subsequent layer growth. With increasing run duration, chlorite grows to well-crystallized, hexagonal platelets up to 10 μm in diameter. The growth is controlled first by the layer growth mechanism and later by the spiral growth mechanism. The first appearance of 14 Å chlorite (Cho and Fawcett, 1986, fig. 3) approximately represents the transition between the earlier three-dimensional nucleation and later layer growth mechanisms. However, there is no apparent distinction in size and morphology between 7 Å and 14 Å chlorites.

The variation in growth mechanism of chlorite with increasing run duration correlates with the trend of decreasing supersaturation in fluid-solid crystallization (Sunagawa, 1981).

Morphology and growth mechanism of cordierite

There are very few descriptions in the literature of the morphology and growth mechanism of cordierite (Venkatesh, 1952). For rapidly grown cordierite crystals in para-lavas (fused shale) from the Bokaro coal field, Venkatesh explained the preferred absorption or growth at corners and edges, and the sluggish growth on the prism face as being due to the different degrees of saturation of atoms at those spots and also probably due to the development of needle-like crystals in the earlier stages.

Cordierite forms larger grains than any other phase found in this study. The cordierite crystals can be divided into two types depending upon the size and morphology; needle-like crystals (Type I) and large (40 to 400 μm) euhedral crystals (Type II).

Type I cordierite

Type I cordierites are acicular or slender prismatic grains, elongated on the c-axis. They are less than 25 μm in length and usually occur as clusters of needles preferentially arranged around the Type II cordierite grains in shorter duration experiments (1 to 28 days at 740°C). With increasing duration, they become more abundant and occur throughout the run product, associated with forsterite and spinel. However, in runs longer than 39 days at 740°C, typical needle-like grains are not observed. They are assumed to disappear with increasing run duration. Therefore, it is apparent that they are a metastable form of cordierite, probably high-cordierite which crystallized prior to the final stable low temperature form. In order to identify the Type I cordierites, Type II cordierites were hand-picked from the run product and the residual portions were X-rayed from 29 to 30° 2θ at a scanning speed of ¼° 2θ/minute (Cu$K\alpha$ radiation). This attempt to measure the distortion index (Δ, Miyashiro, 1957) of Type I cordierite in the cordierite–forsterite–spinel assemblage was not successful because of the poor resolution caused by their small abundance.

Type II cordierite

Type II cordierite occurs as squat or elongate hexagonal shaped prisms which have grown to exceptionally large size. The distortion index (Δ) of Type II cordierites is approximately 0.20, typical of low cordierite.

The size of Type II cordierite grains generally increases with increasing run duration but different sizes varying from 40 μm up to 400 μm are not uncommon even in the same run product. The morphology also does not show

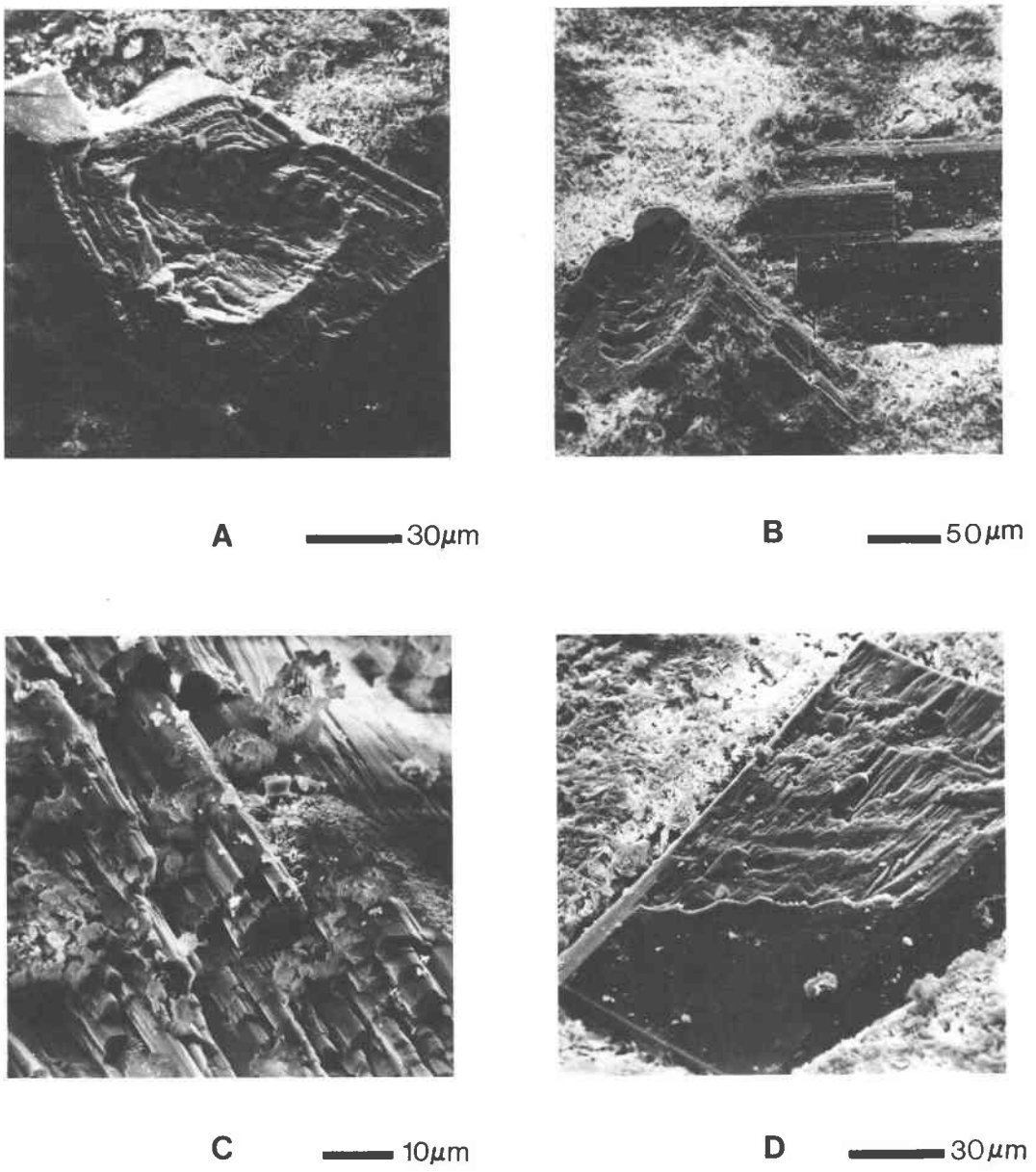

Fig. 3. Growth features of Type II cordierite. (A) Oblique view of cordierite, showing zonal structure. Note the concave structure in the central portion, which may indicate the change in growth mechanism with increasing time (744°, 3 days). (B) Concave structure in the central portion of the basal plane (725°, 36 days). (C) Columnar growth parallel to the c-axis of cordierite. The basal terminations of each hexagonal cordierite is smooth without pits (712°C, 72 days). (D) An oblique section of a well-developed cordierite showing the channel structure (722°C, 9 days).

any systematic change with increasing run duration. These phenomena probably result from the fact that both nucleation and growth have occurred simultaneously. Surface features of the basal planes and prism faces of Type II cordierite are described below.

Basal faces. Structurally controlled pits, zonal structure, concave structure in the central portion and the surface associations of Type I cordierite or talc (?) have all been observed. The general morphology of basal planes develops from anhedral to euhedral with hexagonal forms. In the initial stage of growth, the (001) faces are bounded by so many prism faces that they appear as apparently rounded or circular faces. In the intermediate stage, they exhibit flat and curved prism faces. The final equilibrium shape is well-faceted and consists of lower-index prism faces. According to the Wulff theorem, if the given surface does occur in the equilibrium shape, no hill and valley structure can be stable (Bennema, 1973). However, such a well-developed equilibrium shape has not been encountered

in this study. Most grains are partly bounded by unstable, stepped or curved faces and belong to the intermediate stage of growth.

Surface roughness also shows wide variation. In a few cases, especially in shorter runs, no pits are observed and tabular talc or forsterite cover the cordierite surface. However, the majority of (001) faces show a variable density of pits that are hexagonal, triangular, stretched or irregular shapes which are aligned along particular directions. Rounded pits are also found and appear to have been partially filled by later growth (Fig. 2C). Figure 2D shows skeletal growth of cordierite that results in growth pits intersecting at 60° and 120°. Both of these alignments of pits are further evidence for the structural control of growth.

Areas between pits show smooth, curved or well-faceted surfaces. They are most commonly occupied by multi-faceted surfaces. Many such pits may contain fine grains of spinel or other phases produced during the growth of cordierite (Fig. 2C). This enclosure of fine grains can explain the numerous inclusions of spinel or forsterite that are commonly observed under the polarizing microscope in synthetic cordierite crystals.

Zonal structures are only found rarely in 740°C runs (Fig. 3A). They reflect a faster growth rate parallel to the c-axis than to the (001) plane with increasing run duration.

In the basal plane of some crystals, pits are preferentially concentrated in the central axis of the crystal (Fig. 3B). The central portion, with abundant pits is often coincident with a concave structure but the periphery of these basal planes is usually smoother and lacking in pits. Thus, it is apparent that two different rates or mechanisms have been effective in the formation of (001) plane. These phenomena described above can be explained by analogy with the variation of crystal morphology in solution growth. Sunagawa (1981) analyzed morphological variation as a function of the degree of supersaturation. He noted a progression from (1) dendritic form with curved surfaces and branches (continuous growth), (2) hopper or skeletal morphology (two-dimensional nucleation growth), to (3) bulky form with macroscopically flat surfaces (dislocation-controlled growth), in the order of decreasing degree of supersaturation. Therefore, the basal plane of Type II cordierite might have grown initially by a continuous growth mechanism, followed by a nucleation- or dislocation-controlled mechanism, which is in accordance with the decreasing degree of supersaturation.

Prism faces. Prism faces also show a variation in their surface roughness; smooth, stepped or columnar. The occurrence of apparently smooth vs. stepped faces on different parts of the same crystal may reflect different growth mechanisms. Allen and Fawcett (1982) interpreted the smooth faces as resulting from the faster spreading rate of surface layers than the nucleation rate, and stepped faces from the opposite situation.

Many elongated hexagons appear to grow vigorously in the direction of the c-axis (Fig. 3C). They grow side by side to show columnar or linear features. Generally, the different terminations of elongate pseudohexagons result in an irregular appearance. The individual hexagons are commonly composed of faces with planar terminations. Further growth of these irregular columns may result in stepped and smooth faces.

During growth, pseudohexagonal individuals are not always close-packed but often enclose a series of open channels parallel to the c-axis. They appear to be partly filled by later growth and become discontinuous, as shown in the oblique sections of well-grown cordierites (Fig. 3D). The abundant pits on the (001) face are the consequence of these channel structures, which have been trapped by fast growth and not filled completely by late growth on basal planes.

Also commonly found in longer runs are overgrowths of Type I cordierite and/or tabular rounded grains (talc?) on both basal and prism faces of Type II cordierite. They show no apparent preferred orientation. This phenomenon was also found in natural cordierite by Venkatesh (1952). He described the common development of the needle-like outgrowths that characterize the earlier stages of all rapidly grown cordierite.

Growth mechanism of cordierite

The appearance of cordierite in shorter duration experiments was easily detected by SEM but not found by XRD, since at most only a few grains of Type II cordierite occurred in the initial stage. Type I cordierite was rarely observed and most grains are Type II cordierite with well-defined crystal faces. The growth of cordierite in the initial stage is confined to the surfaces of the experimental charge which were in contact with the sample container. Thus, the absence of Type I cordierite can be explained by the faster growth rate of Type II cordierite and the relatively low nucleation frequency of Type I cordierite in the early stage of cordierite growth.

The formation of Type I cordierite is the result of growth from nuclei, which have grown by the mechanism of three-dimensional nucleation. As they grow in length parallel to the c-axis, they are attached or linked together and aligned parallel to one another to form rod- or pencil-like aggregates. These linked clusters can grow along their sides by successively adding new nuclei or nuclei-clusters. The result is the large euhedral Type II cordierite, elongated along the c-axis.

Type I cordierite also adheres to the surface of Type II cordierite formed in the earlier stages, accelerating the growth of Type II cordierite. Thus, in the appropriate range of time and temperature, three-dimensional nucleation is operating together with the two-dimensional growth of Type II cordierite. The earlier formed crystals grow to a large size due to the heterogeneous nucleation and growth. With increasing duration, no Type I needles are observed on the surface of larger cordierites or in the fine grained matrix. Therefore, the three-dimensional nucleation is not effective and (both Type I and II) cordierite grows by two-dimensional nucleation.

Random distribution of the crystalline size of cordierite

even in the same run product is attributed to the heterogeneous nucleation and growth of cordierite controlled by the sample container. As no attempt was made to overcome the heterogeneous nucleation and growth, a kinetic interpretation of cordierite growth, employing the size of variation with increasing duration (e.g., Kirkpatrick, 1981), is not possible.

This study provides a further illustration of utility of the scanning electron microscope in the hydrothermal experimental studies. The SEM investigations of synthetic chlorite and cordierite have revealed systematic variations in crystal morphologies and growth mechanisms, as a function of experiment duration and temperature. However, our experience has shown that with the starting materials used at the conditions of our experiments, the products are usually too fine grained to determine reaction mechanisms during synthesis.

Acknowledgments

This study represents part of M. Cho's M.Sc. thesis at the University of Toronto. Dr. J. M. Allen and Dr. G. M. Anderson have contributed greatly in discussions during the course of the work. We also thank Mr. G. Gomolka for the technical assistance in SEM work. This research was supported by grants from the Natural Sciences and Engineering Research Council of Canada to J. J. Fawcett and by the H. V. Ellsworth Fellowship in Mineralogy at the University of Toronto, to M. Cho. Reviews of a preliminary version of this manuscript by J. M. Allen, J. V. Chernosky, D. A. Hewitt, T. P. Loomis and J. G. Liou resulted in significant improvements to the presentation.

References

Allen, J. M. and Fawcett, J. J. (1982) Zoisite–anorthite–calcite stability relations in H_2O–CO_2 fluids at 5000 bars: an experimental and SEM study. Journal of Petrology, 23, 215–239.

Baronnet, A. (1972) Growth mechanisms and polytypism in synthetic hydroxl-bearing phlogopite. American Mineralogist, 57, 1272–1293.

Baronnet, A. (1978) Some aspects of polytypism in crystals. Progress in Crystal Growth and Characterization, 1, 151–211.

Bennema, P. (1973) Generalized Herring treatment of the equilibrium form. In P. Hartman, Ed., Crystal Growth: An Introduction, p. 342–357. North-Holland Publications Co., Amsterdam.

Cho, M. and Fawcett, J. J. (1982) Mechanisms and kinetics of the reaction, clinochlore = forsterite + cordierite + spinel + vapour. (abstr.) Transactions of the American Geophysical Union (EOS), 63, 465.

Cho, M. and Fawcett, J. J. (1986) A kinetic study of clinochlore and its high temperature assemblage, forsterite–cordierite–spinel at 2 kbar water pressure. American Mineralogist, 71, 68–77.

Franchini-Angela, M. and Aquilano, D. (1984) Theoretical growth morphology of whewellite $CaC_2O_4 \cdot H_2O$. Physics and Chemistry of Minerals, 10, 114–120.

Kirkpatrick, R. J. (1981) Kinetics of crystallization of igneous rocks. In A. C. Lasaga and R. J. Kirkpatrick, Eds., Reviews in Mineralogy, Vol. 8: Kinetics of Geochemical Processes, p. 321–398. Mineralogical Society of America, Washington, D.C.

Miyashiro, A. (1957) Cordierite–indialite relations. American Journal of Science, 255, 43–62.

Pamplain, B. R. (1975) International Series in the Science of the Solid State, Vol. 6: Crystal Growth. Pergamon Press, New York.

Sunagawa, I. (1977) Natural crystallization. Journal of Crystal Growth, 42, 214–223.

Sunagawa, I. (1981) Characteristics of crystal growth in nature as seen from the morphology of mineral crystals. Bulletin de Minéralogie, 104, 81–87.

Tuttle, O. F. (1949) Two pressure vessels for silicate–water studies. Bulletin of the Geological Society of America, 60, 1727–1729.

Venkatesh, V. (1952) Development and growth of cordierite in para-lavas. American Mineralogist, 37, 831–848.

Verma, A. R. (1953) Crystal Growth and Dislocation. Butterworths Scientific Publications, London.

Manuscript received, December 1, 1983;
accepted for publication, September 9, 1985.